

TABLE OF CONTENTS

	Page
ACKNOWLEDGEMENTS	iii
ABSTRACT (ENGLISH)	iv
ABSTRACT (THAI)	v
LIST OF TABLES	viii
LIST OF FIGURES	ix
ABBREVIATIONS AND SYMBOLS	xii
CHAPTER 1 INTRODUCTION	1
1.1 Overview	1
1.2 Objectives	2
CHAPTER 2 LITERATURE REVIEW	3
2.1 Dental Porcelains	3
2.1.1 Historical perspective	3
2.1.2 Chemical compositions	4
2.1.3 Structures	7
2.1.4 Application in dental field	12
2.2 Leucite	18
2.2.1 Composition and structure	18
2.2.2 Leucite reinforce dental porcelains	21
2.2.3 Phase transformation of leucite reinforce dental porcelains	25
2.2.4 Content and size of leucite reinforce dental porcelains	27
2.3 Zirconia	31
2.3.1 Composition and structure	32

2.3.2 Zirconia reinforced ceramics	33
2.4 Ceramic Nanocomposites	34
2.4.1 Ductile- Phase Toughening	35
2.4.2 Fiber Toughening	35
2.4.3 Transformation Toughening	36
2.4.4 Microcrack Toughening	37
CHAPTER 3 EXPERIMENTAL PROCEDURE	41
3.1 Sample Preparation	41
3.1.1 Powder Preparation	41
3.1.2 Preparation of the specimens	41
3.2 Sample Characterization	47
3.2.1 Phase Analysis	47
3.2.2 Microstructural Analysis	48
3.2.3 Size Analysis	48
3.2.4 Density Analysis	48
3.3 Statistical Analysis	48
CHAPTER 4 RESULTS AND DISCUSSION	51
CHAPTER 5 CONCLUSIONS AND SUGGESTIONS	
FOR FUTURE WORKS	62
5.1 Conclusions	62
5.2 Suggestions for Further Work	62
REFERENCES	63
VITA	76

LIST OF TABLES

Table	Page
2.1 Compositions of household and dental porcelains.	5
2.2 Chemical composition analysis of some commercial dental porcelains.	6
3.1 The firing schemes employed for the production of sample.	42
4.1 Physical properties of dental porcelain ceramics containing varies amount of ZrO ₂ additives.	52
4.2 EDX chemical analysis of dental porcelain ceramics containing various amount of ZrO ₂ additives.	59

LIST OF FIGURES

Figure	Page
2.1 Whiteware compositions composed of clay, feldspar, and silica (quartz).	5
2.2 Structural units of SiO ₄ tetrahedra: (a) diagram of silicate unit with each SiO tetrahedra sharing an oxygen atom, (b) a silicate unit which the silicon atom (Si) is surrounded by four oxygen atoms (oxygen polyhedra) and (c) linked silicate units which form the network in glass.	8
2.3 Two-dimensional presentation of an oxide M ₂ O ₃ in (a) the crystalline form and (b) the glass form.	8
2.4 Reaction between sodium oxide and silica tetrahedral. The sodium oxide contributes one of the non-bridging oxygen ions which interrupt the continuity of the silica network.	10
2.5 Two-dimensional representation of the structure of sodium silicate glass (The structure is shown in a simplified form since only three of the four oxygen ions surrounding each silicon ion are depicted.)	11
2.6 Aluminium in a silicate network (The structure is shown in a simplified form; the true structure is three-dimensional, the AlO ₄ and SiO ₄ groups having tetrahedral configurations.). The alkali metal ion (M ⁺) such sodium maintains electroneutrality.	12
2.7 Applications of dental porcelain-based ceramics: (a) inlay, (b) all ceramic jacket crown and (c) bridge.	13
2.8 Methods of strengthening dental porcelain: (a) enameling of metals, (b) enameling of high strength crystalline ceramics and (c) production of pre-stressed surface layers in dental porcelain via ion-exchange.	14
2.9 In all-ceramic restoration, incidental light is transmitted and partially diffused through. On the other hand, when entering a PFM restoration, light is primarily reflected	17

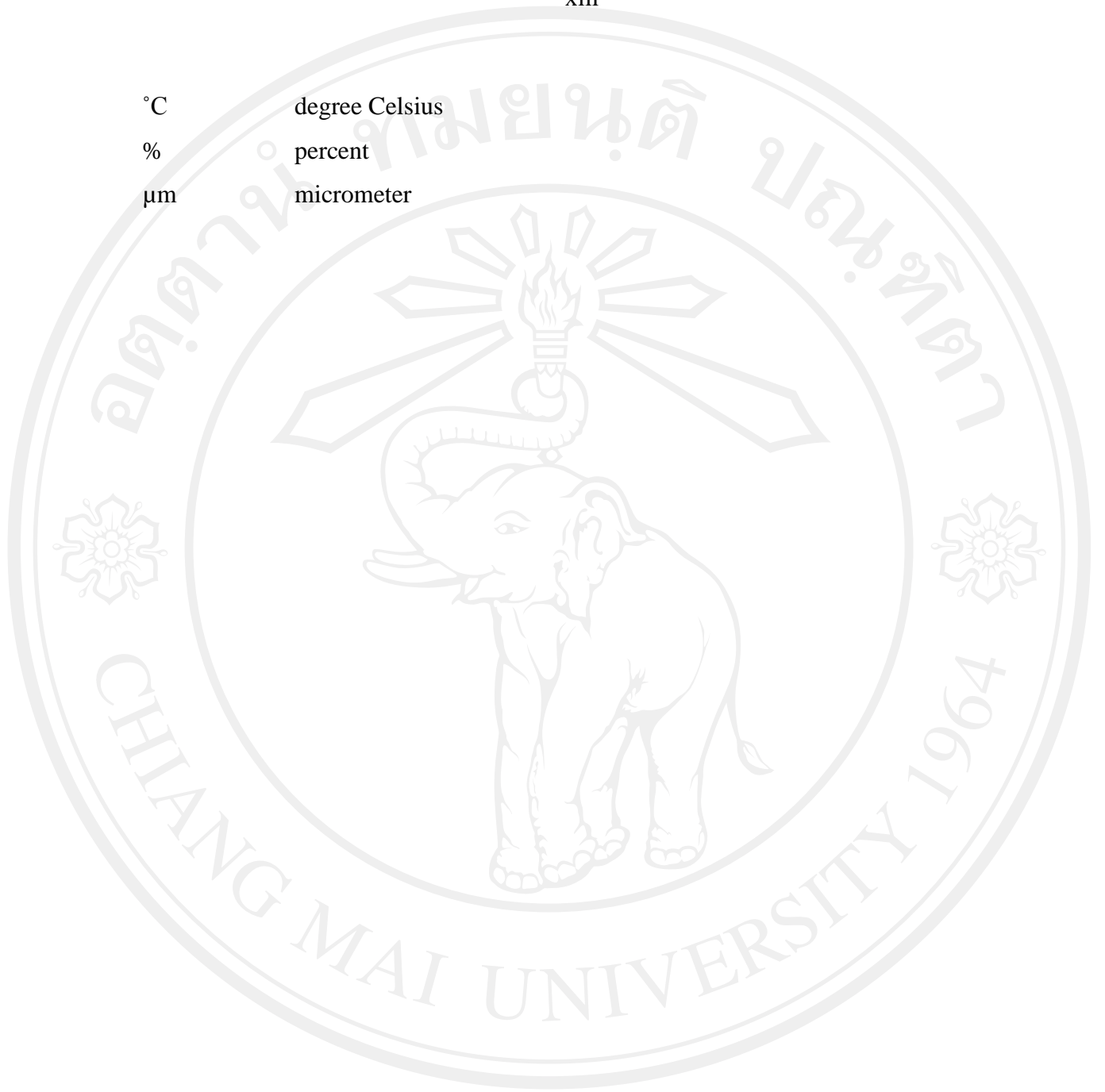
- 2.10 The unit cell of tetragonal leucite (23°C) viewed parallel to {111}. The potassium atoms (spheres) reside along non-intersecting {111} channels; such channels are interconnected via side channels perpendicular to the main channel axis (shown as *lines* radiating from the central K atoms to neighbouring K atoms in adjacent channels; the distances between such K atoms are approximately 4.7 Å). Directions of the side channels are indexed. 20
- 2.11 View parallel to {110} showing the arrangement of potassium atoms and the six-fold tetrahedral rings along the {111} direction. (a) Below T_C , the potassium atoms (spheres) are off-centered with respect to the channel axis (*diagonal line*). (b) At 800°C, in the cubic phase, the potassium atoms are aligned parallel to the (*triad*) channel axis, and the rings assume an undistorted profile. The average distance between the potassium ions parallel to this axis is approximately 6 Å. 21
- 2.12 Position of feldspathic ceramic bodies for denture teeth and for ceramo-metallic restorations in the ternary-phase diagram $K_2O-Al_2O_3-SiO_2$. Phase diagram reprinted by permission of American Ceramic Society. 22
- 2.13 Micrograph of crystalline phase reinforced porcelains; (a) leucite, (b) lithium disilicate, (c) zirconia, and (d) fluoro-apatite. 24
- 2.14 Schematic of microcracks during cooling of porcelain from the glass transition temperature to room temperature. As the porcelain cools down from the firing temperature, the leucite contracts more than the surrounding glass matrix, owing to its higher coefficient of thermal expansion and the cubic-to-tetragonal phase transformation. At some temperature below the glass transition temperature of the glass matrix, the walls of the cracks around the leucite particles separate due to the contraction of the leucite particles. 26
- 2.15 Schematic representation of the three polymorphs of ZrO_2 : (a) cubic, (b) tetragonal, and (c) monoclinic. 33

2.16	Schematic illustrations of toughening mechanisms in ceramic-matrix composites: (a) ductile-phase toughening, (b) fiber toughening, (c) transformation toughening, and (d) microcrack toughening.	37
2.17	(a) Niihara's classification of nanocomposite types, based on matrix grain size and second-phase particle size. (b) A new classification, Kuntz in which the matrix phase is continuously nanocrystalline while the second phase varies, leading to four nanocomposite types.	39
3.1	Flow chart of green sample preparations.	43
3.2	Industrial shaping process of dental porcelain by slip casting technique: (1) pouring slip into the metal mold, (2) excess moisture removing, (3) surface flattening, (4) unpacking, (5) green specimen, and (6) sintered specimens.	44
3.3	Vacuum furnace (for reducing sample porosity after sintering process).	45
3.4	Flow chart of the specimen preparations.	46
3.5	X-ray diffractometer.	49
3.6	Scanning electron microscope, equipped with EDX analyzer.	49
3.7	Digital scale was used for measuring density by the Archimedes principle.	50
4.1	X-ray diffraction patterns of dental porcelain doped with various amount of ZrO_2 additive.	53
4.2	Enlarge X-ray diffraction of patterns of dashed box in Fig. 4.1	54
4.3	SEM micrograph of dental porcelain ceramics with various amount of ZrO_2 additive.	57
4.4	Representative (a) SEM micrograph of 20 wt% ZrO_2 modified sample and their corresponding EDX analysis, indicating the chemical compositions of (b) glassy matrix, (c) leucite and (d) ZrO_2 phases, respectively.	59
4.5	The variation of leucite content (■) and density (▲) of the porcelain based samples as a function of the amount of ZrO_2 additive.	61

ABBREVIATIONS AND SYMBOLS

Å	Angstrom
ANOVA	Analysis of Variance
ASTM	American Society for Testing Materials
cm	centimeter
EDX	Energy Dispersive X-ray Spectrometry
g	gram
GPa	gigapascal
g/cm ³	gram per cubic centimeter
ISO	International Organization for Standardization
JCPDS	Joint Committee for Powder Diffraction Standards
λ	Lambda
\ln	Logarithm
K_{IC}	fracture toughness
kV	kilovolt
m	Weibull moduli
mA	miliampare
min	minute
mm	millimeter
mm ³	Cubic Millimeter
MPa	megapascal
N	Newton
nm	nanometer
pm	picometer
PVA	Polyvinyl Alcohol
SEM	Scanning Electron Microscopy
vol%	percent volume
wt%	percent weight
XRD	X-ray Diffraction

°C degree Celsius
% percent
μm micrometer



ลิขสิทธิ์มหาวิทยาลัยเชียงใหม่
Copyright © by Chiang Mai University
All rights reserved